Lawrence Berkeley National Laboratory
Recent Work

Title
CLASSICAL S-MATRIX FOR LINEAR REACTIVE COLLISIONS OF H + C12

Permalink
https://escholarship.org/uc/item/4f7879hd

Authors
Rankin, C.C.
Miller, W.H.

Publication Date
1971-05-01

RECEIVED
LAWRENCE
RADIATION LABORATORY

LIBRARY AND
DOCUMENTS SECTION

CLASSICAL S-MATRIX FOR LINEAR REACTIVE COLLISIONS OF H + Cl_2

C. C. Rankin and W. H. Miller

May 1971

LAWRENCE RADIATION LABORATORY
UNIVERSITY of CALIFORNIA BERKELEY

UCRL-20583

DISCLAIMER

CLASSICAL S-MATRIX FOR LINEAR REACTIVE

COLLISIONS OF H + Cl_2 [*]

C. C. Rankin and W. H. Miller[‡]

Inorganic Materials Research Division,
Lawrence Radiation Laboratory,
Department of Chemistry,
University of California,
Berkeley, California 94720

ABSTRACT

Classical trajectories are computed for linear H + Cl_2 collisions
and used to construct the classical limit of the S-matrix for reactive
and non-reactive transitions between individual quantum states. An
interesting feature of this system is that both "direct" and "complex"
mechanisms participate in the collision dynamics. The two mechanisms
contribute additively to individual S-matrix elements, and within a
"random phase approximation" for the complex contribution it is seen that
they also contribute additively to the transition probability. The com-
plex contribution to a transition probability is strictly classical, but
interference structure may be prominent in the direct contribution.

I. Introduction

It is well-recognized now that at least the gross features of atomic
and molecular collision dynamics are accurately described by classical
mechanics. The facility with which classical trajectories can be com-
puted, with averaging over various initial conditions (usually by Monte
Carlo methods), and used to generate averaged collision properties (thermal
rate constants for chemical reaction, the average energy transfered be-
tween internal and translational degrees of freedom, etc.) is evidenced
by the large amount of such work currently being reported.[1] For the
relatively simple atom-diatom and diatom-diatom collision systems this
strictly classical approach has almost reached the stage of being a tool
for the analysis of experimental results.

Motivated by the way classical mechanics has been used within a
quantum mechanical framework to treat elastic atom-atom scattering,[2] we
have recently shown[3] how exact classical mechanics (i.e., numerically
computed trajectories) for a complex collision system (i.e., one with
internal degrees of freedom, such as A + BC) can be used to construct
the classical limit of the quantum mechanical S-matrix (the "classical
S-matrix") describing transitions between individual quantum states of
the collision partners.[4] Use of classical mechanics to construct such
transition, or scattering amplitudes (rather than transition probabili-
ties or cross sections directly) means that the quantum principle of
superposition is incorporated, and, just as in elastic scattering, the
interference features so obtained seem to be the chief contribution of
quantum mechanics. It is often possible to analytically continue the
interference structure into classically forbidden domains so that

transitions which proceed by tunneling can also be treated by classical mechanics[5] (analogous to the WKB treatment of tunneling in one-dimensional problems). The general conclusion of the examples studied thus far is that classical dynamics, appropriately used, is capable of much greater detailed accuracy than may have been previously suspected.

This paper reports results of the classical S-matrix approach applied to a linear reactive atom-diatom collision, $H + Cl_2 \rightarrow HCl + Cl$; the particular potential surface used, collision energies employed, etc., are those for which Miller and Light[6] have recently reported quantum mechanical results. Section II presents the details of the classical S-matrix approach as it applies to the linear reactive A + BC system, and Section III discusses the numerical results for $H + Cl_2$. The most interesting new feature seen in this system, other than that of reaction itself, is the participation of two distinct collision mechanisms; some trajectories are "direct", whereas others lead to "complex formation" and are thus quite complicated. It is seen in Section III how "direct" and "complex" mechanisms contribute to the S-matrix and to the net transition probability.

II. <u>Classical S-Matrix for Linear Reactive A + BC Collisions.</u>

The general expressions for the classical S-matrix have been given in reference 3; here the notation and results are summarized as they apply to the linear reactive A + BC collision. Figure 1 shows the coordinates, r_a and R_a being the vibrational and center-of-mass translational coordinates for initial arrangement a(A + BC), and r_c and R_c being analogous coordinates for arrangement c(AB + C); we refer to these as the cartesian coordinates for arrangements a and c. A linear transformation relates the cartesian coordinates of the two arrangements

$$\begin{pmatrix} R_c \\ \\ r_c \end{pmatrix} = \begin{pmatrix} \dfrac{A}{A+B} & \dfrac{B(A + B + C)}{(A + B)(B + C)} \\ \\ 1 & -\dfrac{C}{B + C} \end{pmatrix} \begin{pmatrix} R_a \\ \\ r_a \end{pmatrix} \quad , \tag{1}$$

where A, B and C are the masses of the individual atoms.

The classical Hamiltonian, in terms of the cartesian coordinates and momenta of arrangement a, is

$$H(P_a, p_a, R_a, r_a) = P_a^2/2\mu_a + p_a^2/2m_a + V^{tot}(r_a, R_a) \tag{2}$$

where the internal and translational reduced masses are

$$m_a = BC/(B + C)$$

$$\mu_a = A(B + C)/(A + B + C) \quad ;$$

the Hamiltonian can be similarly expressed in terms of the cartesian coordinates and momenta of arrangement c. The internal (vibrational) potentials in arrangements a and c are

$$v_a(r_a) = \lim_{R_a \to \infty} V^{tot}$$

$$v_c(r_c) = \lim_{R_c \to \infty} V^{tot} \quad ;$$

the potential surface of Miller and Light[6] is such that these vibrational potentials are Morse functions

$$v(r) = D[e^{-2\alpha(r-r_o)} - 2e^{-\alpha(r-r_o)}] \quad , \tag{3}$$

where the Morse parameters D, α, and r_o correspond to diatomic molecule BC for arrangement a and AB for arrangement c.

To effect quantization in the asymptotic regions one carries out a canonical transformation of the internal degree of freedom from cartesian variables r and p to angle-action variables q and n. The generator of this canonical transformation[7], of the F_2-type, is given by

$$f_2(r,n) \equiv \pm \int_{r_<}^{r} dr' \left\{ 2m[\epsilon(n) - v(r')] \right\}^{1/2} , \qquad (4)$$

which for the Morse potential of Equation (3) becomes

$$f_2(r,n) = \pm \frac{k}{2} \left\{ -(-z^2 + 2z - \lambda^2)^{1/2} + \cos^{-1}[(z-1)(1-\lambda^2)^{-1/2}] \right.$$
$$\left. - \lambda \cos^{-1}[(z-\lambda^2)(1-\lambda^2)^{-1/2} z^{-1}] \right\} , \qquad (5)$$

where

$$z = \exp[-\alpha(r-r_o)]$$
$$k = 2(2mD)^{1/2}/a$$
$$\lambda = (1 - \frac{2n+1}{k})$$
$$\pm = \text{sign of } p .$$

In terms of the angle-action variables the internal Hamiltonian (for either arrangement), $p^2/2m + v(r)$, becomes the semiclassical (Bohr-Sommerfield) eigenvalue function (which, for the Morse oscillator, happens to be identical to the quantum eigenvalue expression)

$$\epsilon(n) = -D(1 - \frac{2n+1}{k})^2 , \qquad (6)$$

and the cartesian variables r and p are given in terms of q and n by

$$r(q,n) = r_o + a^{-1} \log \left\{ \lambda^{-2}[1 - (1 - \lambda^2)^{1/2} \cos q] \right\} \qquad (7)$$

$$p(q,n) = m \, \epsilon'(n) \frac{\partial r(q,n)}{\partial q} \qquad , \qquad (8)$$

where λ is given below Equation (5). All of the expressions in this paragraph apply equally well for either arrangement a or c.

It actually turns out to be most convenient[8] to carry out the numerical integration of Hamilton's equations in the cartesian variables r, p, R, and P rather than the angle-action variables q, n, R, and P. Initial conditions, however, are specified in terms of angle-action variables; i.e., one specifies initial conditions in angle-action variables, transforms to cartesian variables and computes the trajectory, and then transforms back to angle-action variables in the final asymptotic region. At fixed total energy E, therefore, one specifies initial values q_1^a and n_1^a for the initial arrangement (subscripts 1 and 2 refer to initial and final times t_1 and t_2, respectively; when it is necessary to specify the time subscript, the arrangement index $\gamma = a$, c is written as a superscript), and then initial values of all the cartesian variables are given by

$$R_1^a = \text{large}$$
$$P_1^a = -\left\{ 2\mu_a[E - \epsilon(n_1^a)] \right\}^{1/2}$$
$$r_1^a = r(q_1^a, \, n_1^a)$$
$$p_1^a = p(q_1^a, \, n_1^a) \quad ,$$

where the functions $\epsilon(n)$, $r(q,n)$, and $p(q,n)$ are given by Equations (6) - (8).

With these initial conditions Hamilton's equations, with the

Hamiltonian of Equation (2), are numerically integrated until one of the asymptotic regions is reached. The final vibrational energy is ϵ_γ,

$$\epsilon_\gamma \equiv p_\gamma^2/2m_\gamma + v_\gamma(r_\gamma) \quad , \tag{9}$$

where γ = a(non-reactive) or c(reactive); the final vibrational quantum number is found by inverting the eigenvalue function in Equation (6)

$$n(\epsilon) = -1/2 + (1/2)k[1 - (-\epsilon/D)^{1/2}], \tag{10}$$

so that n_2^γ is given by

$$n_2^\gamma = n(\epsilon_\gamma) \quad , $$

with ϵ_γ given by Equation (9), and γ = a or c.

This final vibrational quantum number, as a function of the initial angle-action variables of the internal degree of freedom, $n_2^\gamma(q_1^a, n_1^a)$, is the fundamental classical trajectory function which is required. It plays precisely the same role here as in the case of non-reactive vibrational excitation[9], except that now there is a reactive and a non-reactive branch; i.e., since a particular trajectory is either reactive or non-reactive, there will be one range of q_1^a which gives non-reactive trajectories and thus determines $n_2^a(q_1^a, n_1^a)$, and another range of q_1^a which give reactive trajectories and thus determines $n_2^c(q_1^a, n_1^a)$.

To construct the classical S-matrix for a particular $n_1^a \to n_2^\gamma$ translation, therefore, one finds all roots of the trajectory relation

$$n_2^\gamma(q_1^a) = n_2^\gamma \quad , \tag{11}$$

where n_1^a is fixed (and not explicitly indicated as an argument of the

trajectory function) and where n_2^γ on the RHS of Equation (11) is an integer. The classical S-matrix for the $n_1^a \to n_2^\gamma$ transition is thus

$$S_{n_2^\gamma, n_1^a} = \sum \left[2\pi \left(\frac{\partial n_2^\gamma}{\partial q_1^a} \right)_{n_1^a} \right]^{-1/2} \exp\left[i\phi(n_2^\gamma, n_1^a) \right] , \tag{12}$$

where $\gamma = a$(non-reactive) or c(reactive), and where the phase ϕ is specified below; the sum is over all the roots of Equation (11). The transition probability is the square modulus of the S-matrix element

$$P_{n_2^\gamma, n_1^a} = \left| S_{n_2^\gamma, n_1^a} \right|^2 . \tag{13}$$

To construct the phase associated with a particular trajectory, be it reactive or non-reactive, it is useful to take cognizance of the fact that the canonical transformation from cartesian variables (r_a, R_a, p_a, P_a) of arrangement a to cartesian variables (r_c, R_c, p_c, P_c) of arrangement c is a _point_ canonical transformation - i.e., the coordinates r_c and R_c are expressible in terms of the coordinates r_a and R_a alone and do not involve the monenta p_a and P_a (see Equation (1)). The F_1-type generator for a point canonical transformation, however, is identically _zero_.[10] The phase of the S-matrix in the coordinate representation of the cartesian variables is therefore given by

$$\phi(r_2^\gamma \ R_2^\gamma, r_1^a \ R_1^a) = \int_{t_1}^{t_2} dt \ P_a(t) \dot{R}_a(t) + p_a(t) \dot{r}_a(t) \tag{14a}$$

$$= \int_{t_1}^{t_2} dt \ P_c(t) \dot{R}_c(t) + p_c(t) \dot{r}_c(t) , \tag{14b}$$

whether $\gamma = a$ _or_ c. The fact that Equation (14a) and Equation (14b) are

equal is a result of the fact that this "rearrangement transformation" is a point canonical transformation; i.e., according to the general transformation principles established in reference 3, Equation (14b) should have added to it the term $F_1(r_1^\gamma R_1^\gamma, r_1^a R_1^a)$ which results from the rearrangement, but, as noted, this generator is identically zero.

The phase of the classical S-matrix in the "quantum number representation" (i.e., the momentum representation of the angle-action variables) is then obtained by carrying out canonical transformations in the initial and final asymptotic regions from the coordinate representation of cartesian variables to the momentum representation of angle-action variables; the generator for this transformation is

$$F_2(r\,R,\,n\,P) = PR + f_2(r,n) \,, \tag{15}$$

where f_2 is given by Equation (5). Thus the phase $\phi(n_2^\gamma, n_1^a)$ in Equation (12) is

$$\phi(n_2^\gamma, n_1^a) = P_1^a R_1^a + f_2(r_1^a, n_1^a) - P_2^\gamma R_2^\gamma - f_2(r_2^\gamma, n_2^\gamma)$$
$$+ \int_{t_1}^{t_2} dt\, 2T, \tag{16}$$

where the integrand of the integral over time is twice the total kinetic energy expressed in the cartesian variables of either arrangement

$$2T = P_a \dot{R}_a + p_a \dot{r}_a$$
$$= P_a^2/\mu_a + p_a^2/m_a \quad ,$$

or the same with $a \to c$.

The phase is conveniently computed together with $r_a(t)$, $R_a(t)$, $p_a(t)$, $P_a(t)$ by introducing an additional first order differential equation for the function $\chi(t)$,

$$\dot{\chi}(t) = P_a \dot{R}_a + p_a \dot{r}_a,$$

with initial condition

$$\chi(t_1) = P_1^a R_1^a + f_2(r_1^a, n_1^a) \; ;$$

at the end of the trajectory, with $\chi(t_2)$, n_2^γ, etc., determined, the phase of the S-matrix is given by

$$\phi(n_2^\gamma, n_1^a) = \chi(t_2) - P_2^\gamma R_2^\gamma - f_2(r_2^\gamma, n_2^\gamma) \; ,$$

for $\gamma = a$(non-reactive) or c(reactive).

In concluding this Section it should be observed that there are actually no inconveniences or special complications which enter the treatment due to the possibility of rearrangement channels. This is in marked contrast to the purely quantum situation where the complexity is considerably increased due to the fact that the coupled channel Schrodinger equations become integro-differential equations when rearrangement channels are included.[11] Classically, on the other hand, reactive trajectories are no more difficult than non-reactive ones, and it has been seen above that construction of the classical S-matrix is likewise no more difficult in the case of reaction.

III. Results for H + Cl_2

The potential surface for this system is that which has been devised by Rankin and Light[12] but with the potential parameters used by Miller

and Light[6] in their recent quantum mechanical computations; two values
for the total energy are considered,[13] 0.3 eV and 0.1 eV above the value
of the potential at the saddle point. At the higher energy (0.3 eV) vi-
brational states 0-5 are open in the initial arrangement (Cl_2), and
states 0-7 are open in the final arrangement (HCl); at 0.1 eV total
energy states 0-2 and 0-6 are open in the initial and final arrangements,
respectively.[14]

Figure 2 shows a typical classical trajectory function $n_2^r(q_1^a, n_1^a)$
for E = 0.3 eV, $n_1^a = 0$, and with the potential parameters of Table II,
reference 6. There is one interval of q_1^a in which the function is quite
smooth and well-behaved (all of these trajectories being reactive) and
another in which it is exceedingly complicated - here the computed points
are shown directly, and no attempt is made to draw in the continuous
segments. Varying the initial phase q_1^a only slightly in this latter
interval causes the trajectory to change from reactive to non-reactive,
or vice-versa, and causes large changes in the final vibrational quantum
number; all energetically accessible vibrational states are reached by
trajectories in this interval.

From these features, as well as by direct inspection of the trajec-
tories and the collision times, one concludes that this complicated
structure is due to multiple collisions (in classical language), or the
formation of a collision complex (in quantum language). This at first
seems surprising, for the potential is not "attractive" in the ordinary
sense; i.e., if one follows the "reaction path" from H + Cl_2 to HCl + Cl, the
potential energy increases monotonically up to the saddle point and then
decreases monotonically. Complex trajectories arise because of a "pinch"

in the direction perpendicular to the reaction coordinate both before and after the saddle point region itself. The situation is analogous to traveling through a broad canyon with narrow entrance and exit valleys.

Individual classical S-matrix elements are constructed by the procedure discussed in Section II. For the $0 \to 5$ reactive transition, for example, the roots of Equation (11) are indicated graphically by the intersection of the horizontal dotted line with the reactive branches of the classical trajectory function. It is seen that there are two "direct" trajectories and many "complex" trajectories which contribute to the $0 \to 5$ reactive transition, so that the classical S-matrix element is

$$ S = p_1^{1/2} \exp(i\phi_1) + p_2^{1/2} \exp(i\phi_2) + \sum_{k=3} p_k^{1/2} \exp(i\phi_k) \quad (17) $$

$$ = S_{direct} + S_{complex} \quad ; \quad (18) $$

i.e., direct and complex mechanisms contribute additively to the S-Matrix. The two phases ϕ_1 and ϕ_2 associated with the direct trajectories are of the same order of magnitude ($|\phi_1 - \phi_2| \leq \pi$), but the phases ϕ_k for the complex trajectories all differ from ϕ_1 and ϕ_2, and from each other, on the order of several multiples of 2π. (This is due to the extra phase accumulated along the trajectory during the life of the collision complex.) In the transition probability,

$$ P = |S|^2 \quad , \quad (19) $$

therefore, interference terms between different complex trajectories, and between complex and direct trajectories, tend to average (upon summing

over all the complex trajectories) to zero. This gives

$$P = p_1 + p_2 + 2(p_1 p_2)^{1/2} \sin(\phi_2 - \phi_1) + \sum_{k=3} p_k \qquad (20)$$

$$= P_{direct} + P_{complex} \quad ;$$

i.e., within this "random phase approximation" for the phase of the com-
plex trajectories the contribution of direct and complex mechanisms to
the transition probability is also additive. Furthermore, the complex
contribution is strictly classical and can be conveniently determined,
for example, by Monte Carlo methods (or any other space-filling method
of sampling). Even simpler than this, one would expect a statistical
approximation[15] to describe the complex contribution adequately.

It is not necessary, therefore, to find the many roots to Equation
(11) which are associated with complex trajectories. Within the
"averaged classical" approach used previously[16], and which is equivalent
to a Monte Carlo treatment, one determines the complex contribution to
the transition probability as

$$P_{n_2^\gamma, n_1^a}(complex) = (\Delta q_c / 2\pi)(m/N) \qquad (21)$$

where Δq_c is the width of the q_1^a interval which leads to complex forma-
tion, N is a number of trajectories computed at equally spaced q_1^a values
in the interval Δq_c, and m is the number of such trajectories for which
the final vibrational quantum number is in the interval $(n_2^\gamma - 1/2, n_2^\gamma + 1/2)$.
The statistical approximation to this complex contribution is

$$P_{n_2^\gamma, n_1^a}(complex) = (\Delta q_c / 2\pi)/(N_c + N_a) \quad , \qquad (22)$$

where Δq_c is as above, and N_c and N_a are the number of reactive and non-reactive states which are classically accessible from the initial state n_1^a. This latter approximation thus assumes that all classically allowed final states are equally likely to be formed from the collision complex.

Figure 3 shows the numerical results for total energy $E = 0.3$ eV and the potential parameters of Table II, reference 6. The uniform semiclassical expression[9] was used for the direct part of the transition probability rather than the "primitive" semiclassical form in Equation (20). Classically forbidden transitions were treated by expanding the trajectory function in a power series about its extrema to sufficiently high order than additional terms did not affect the complex roots thus obtained[5]; in most cases their contribution was actually negligible in comparison to that from complex formation.

For each initial state $n_1^a = 0$, 1, and 2, non-reactive transitions occur only via complex formation, and reactive transitions have a contribution from both direct and complex mechanisms. For $n_1^a = 0$ a 100 trajectories were computed at equally spaced points in the interval Δq_c which led to complex formation, and the complex contribution to each transition was determined by Equation (21). The dashed line in Figure 3 shows the non-reactive transition probabilities which result from this treatment, and it is seen that they are roughly independent of the final quantum number; i.e., the statistical approximation (Equation (22)), which would give all the non-reactive transition probabilities as $(\Delta q_c/2\pi)/14 \simeq 0.035$, is actually not too bad. The actual distribution into final states is seen to favor the smaller and larger quantum numbers somewhat. The complex contribution to reactive transitions is similar.

Since the statistical approximation for the complex contribution is reasonably accurate for $n_1^a = 0$, it was used for the cases $n_1^a = 1$ and 2 in Figure 3; this simplifies matters considerably, since only the boundaries of Δq_c are thus required. The value of the transition probability to final quantum number 0 in each case shows the value that complex formation contributes to each transition probability, reactive and non-reactive.

For $n_1^a = 2$ in Figure 3, one sees prominent interference structure in the reactive transition probabilities similar to that seen in previous studies.[9] A strictly classical treatment of the direct contribution would, of course, miss this feature.

A brief survey was made of the case E = 0.3 eV with the potential parameters of Tables I and III of reference 6. With the parameters of Table III and $n_1^a = 0$, all trajectories were direct (i.e., no complex formation) and reactive, and the final vibrational quantum numbers were typically smaller than those for the potential parameters of Table II. With the potential parameters of Table I and $n_1^a = 0$, the region of complex formation was greater than that for the parameters of Table II.

Finally, the cases E = 0.1 eV with the potential parameters of Tables II and III, reference 6, were also examined briefly in order to compare some features with the quantum results. The classical trajectory function $n_2^\gamma(q_1^a, n_1^a)$ was computed for $n_1^a = 0$, 1 and 2, and the total reactive probability was determined in a strictly classical approximation,

$$P_{reactive} \simeq \Delta q_{reactive}/2\pi \ .$$

For the potential parameters of Table II the classical values were approximately 0.90, 0.75, and 0.80, for $n_1^a = 0$, 1, 2, respectively, compared to the corresponding total reactive probability of Miller and

Light[6] of 0.81, 0.28, and 0.04. For the parameters of Table III the classical values were 1.00, 0.70, and 0.60, compared to the quantum values[6] 0.87, 0.52, and 0.13. These quantum and classical results are thus in rather poor agreement even at this rather gross level. The reason for the lack of agreement is not completely clear.

One possible factor contributing to the disagreement is the fact that complex formation appears prominently in the classical dynamics. Without the inclusion of a number of closed channels in the quantum calculation, it seems doubtful that a coupled-channel treatment can describe this dynamical feature. It is well-known, for example, that Feshbach resonances (a type of complex formation) which appear in the scattering of an electron from a hydrogen atom[17] cannot appear in a coupled-channel description which retains only the open channels.

Before a detailed comparison of individual transition probabilities obtained semiclassically and quantum mechanically could be possible, it would also be necessary to transform the quantum results from the harmonic oscillator basis to the physically meaningful basis of Morse oscillator states. Thus,

$$S_{n_2,n_1} = \sum_{N_1,N_2} < n_2|N_2 > \, S_{N_2,N_1} \, < N_1|n_1 > ,$$

where $|N>$ and $|n>$ are harmonic and Morse states, respectively, S_{N_2,N_1} is the S-matrix in the harmonic basis obtained in reference 6, S_{n_2,n_1} is the physically meaningful S-matrix, and $< n|N >$ is the overlap between harmonic and Morse states.

IV. Summary and Conclusions.

With this particular system it has been seen that both "direct" and "complex" collision mechanisms can be operative essentially simultaneously. Furthermore, direct and complex mechanisms contribute additively to the S-matrix and, within the "random phase approximation" to the complex contribution, they also contribute additively to the transition probability. The complex contribution to the transition probability is strictly classical, but interference terms between direct trajectories can be quite prominent.

Whether this situation is typical, or an artifact of this particular potential surface, is not known at this time. There are obviously many processes which take place wholy by direct mechanisms and others which proceed wholy by complex formation. Just how often it arises that a process has significant contributions from direct and complex mechanisms is a question that will most likely be answered experimentally before it is theoretically.

References

1. Some of the most recent work of this type is (a) J. van de Ree and J. G. R. Okel, *J. Chem. Phys.*, 54, 589 (1971); (b) J. Lorenzen and L. M. Raff, *ibid*, 54, 674 (1971); (c) J. T. Muckerman, *ibid*, 54, 1155 (1971); (d) R. L. Thommarson, G. C. Berend, and S. W. Benson, *ibid*, 54, 1313 (1971); (e) R. L. Jaffe and J. B. Anderson, *ibid*, 54, 2224 (1971).

2. K. W. Ford and J. A. Wheeler, *Ann. Phys.*, (N.Y.) 7, 259, 287 (1959); for a more recent review of these procedures, see R. B. Bernstein, *Adv. Chem. Phys.*, 10, 75 (1966).

3. W. H. Miller, *J. Chem. Phys.*, 53, 1949 (1970).

4. This classical S-matrix approach may be correctly viewed as an extension of the Old Quantum Theory to the field of scattering. The feeling had previously been that "all collision phenomena lie outside the scope of the [old quantum] theory" (A. Messiah, *Quantum Mechanics*, Wiley, N.Y., 1961, p. 40). The pinnacle of The Old Quantum Theory applied to eigenvalue problems is the treatise by M. Born, *The Mechanics of The Atom*, Ungar, N.Y., 1960. Marcus [R. A. Marcus, *Chem. Phys. Lett.*, 7, 525 (1970), *J. Chem. Phys.*, to be published.] has made important contributions by a different approach than that is reference 3, although many of the physical

ideas underlying the independent developments are the same.

5. W. H. Miller, Chem. Phys. Lett., 7, 431 (1970).

6. G. Miller and J. C. Light, J. Chem. Phys., 54, 1643 (1971).

7. Constructing the generator of the angle-action variable transformation is equivalent to solving the classical equations of motion for the isolated internal degree of freedom. This is the classical equivalent of the necessity in quantum mechanics of first solving for the eigenstates of the internal Hamiltonian, in terms of which a coupled channel expansion may then be formulated.

8. Since the potential surface for the $H + Cl_2$ system is specified in "natural collision coordinates" (see reference 12), it was actually simpler in this special case to carry out the numerical integration directly in these coordinates. In the asymptotic regions these coordinates become the cartesian coordinates (r_a, R_a) or (r_c, R_c), so that all the other details of the procedure are just as discussed in this Section.

9. W. H. Miller, J. Chem. Phys., 53, 3478 (1970).

10. This fact is implicit in the equations on p. 244 of H. Goldstein, Classical Mechanics, Addison-Wesley, Reading, Mass., 1950.

11. W. H. Miller, J. Chem. Phys., 50, 407 (1969). See also, G. Wolken, Ph.D. thesis, Harvard University, 1971.

12. C. C. Rankin and J. C. Light, J. Chem. Phys., 51, 1201 (1969).

13. The intention of this present paper was to compare results of the classical S-matrix approach to the quantum mechanical results of reference 6 which quote the energy as 0.3 eV. This was a misprint (J. C. Light, private communication), however, the actual value

being 0.1 eV.

14. Since a harmonic oscillator basis was used for the vibrational states in the coupled channel expansion of reference 6, the n=6 vibrational state of HCl was not open.

15. P. Pechukas, J. C. Light, and C. C. Rankin, J. Chem. Phys., 44, 794 (1966). In W. H. Miller, J. Chem. Phys., 52, 543 (1970) it is shown how the usual statistical approximation, and extensions thereof, result in the case of complex formation.

16. W. H. Miller, J. Chem. Phys., 54, 15 June 1971.

17. P. G. Burke, Adv. Atom. Mol. Phys., 4, 173 (1968).

Figure Captions

1. The vibrational and translational coordinates which pertain to arrangement a (A + BC) and arrangement c (AB +C).

2. The final vibrational quantum number (solid line and solid points for reactive trajectories, open points for non-reactive trajectories) as a function of the initial phase of vibration. The initial vibrational quantum number is $n_1 = 0$, the total energy (referred to the potential energy at the saddle point) is 0.3 eV, and the potential parameters are those of Table II, reference 6. The horizontal dotted line at $n_2 = 5$ indicates the graphical solution for the roots of Equation (11).

3. Transition probabilities from initial vibrational states 0(bottom), 1, and 2 (top) of Cl_2 to various final vibrational states n. The points connected by the solid line are reactive transitions (final diatom = HCl), and the points connected by the dashed line in the bottom figure are non-reactive transitions (final diatom = Cl_2). The total energy and potential parameters are the same as those for Figure 2. For initial states 1 and 2 the statistical approximation (see Section III of the text) was used to obtain the complex contribution to each transition probability and the value of the transition probability to find state 0 in the figure is the value of the complex contribution to each final state, reactive and non-reactive.
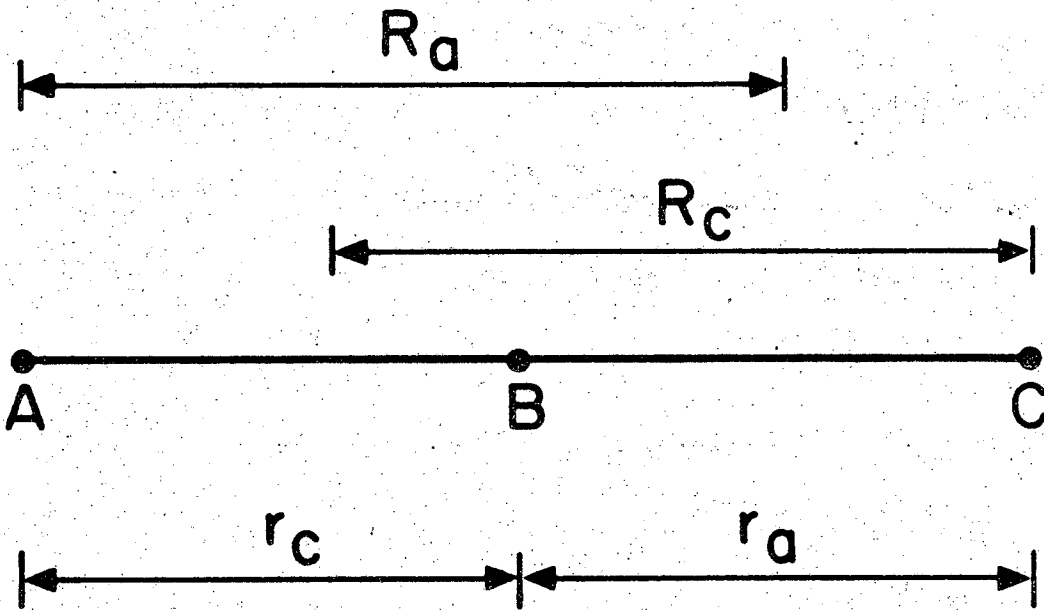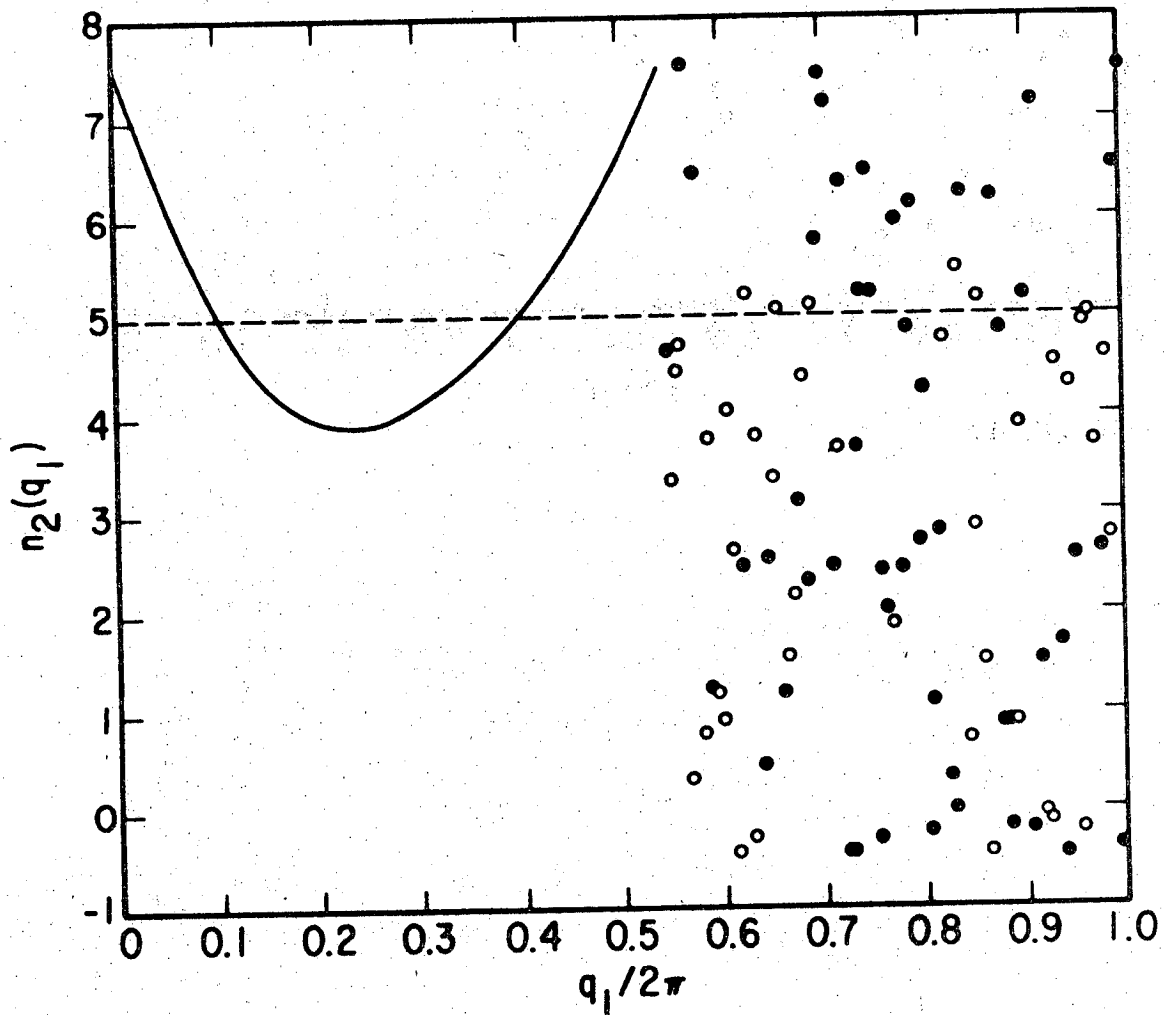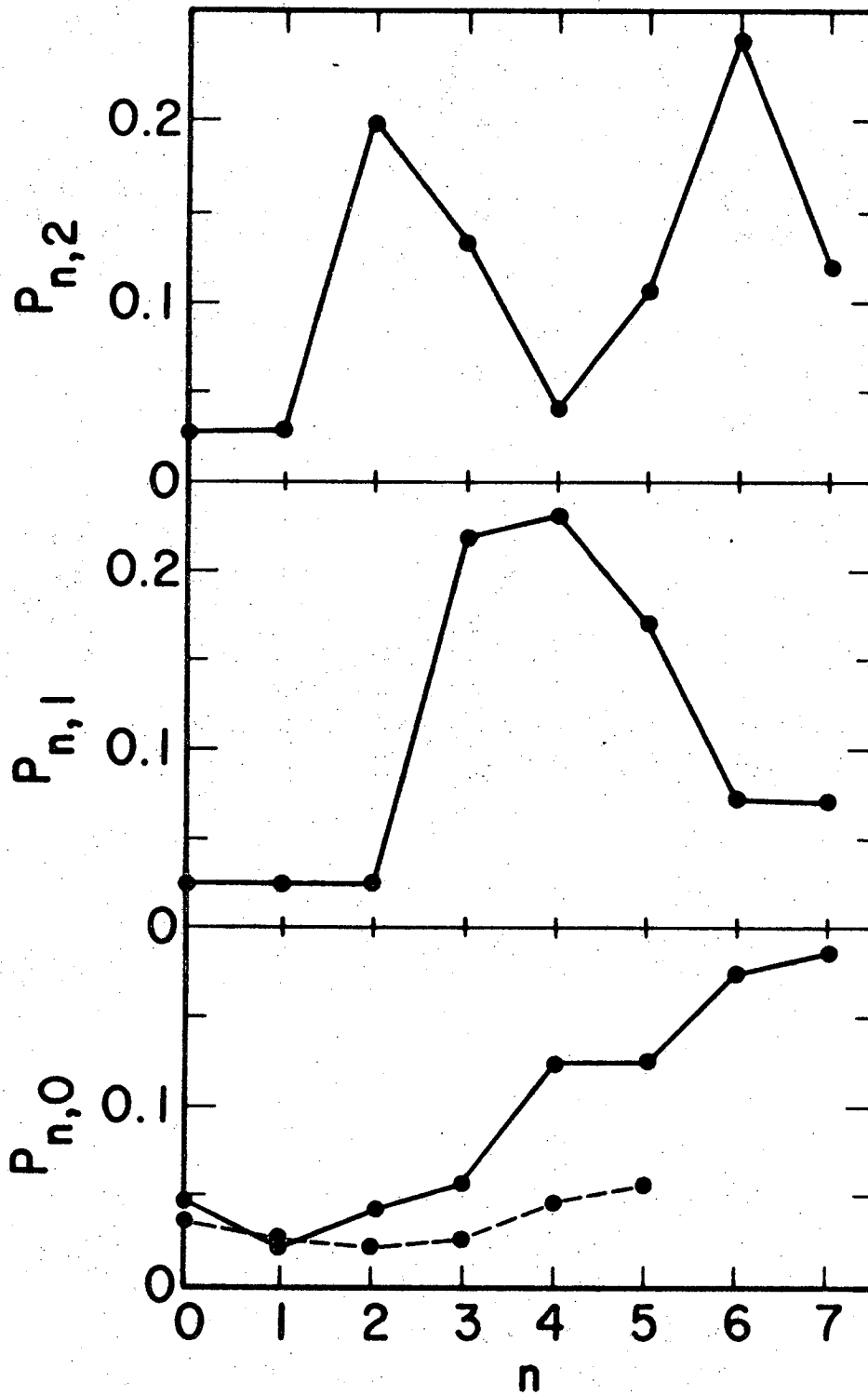
Figure 1.

XBL 712-6501

Figure 2.

XBL715-6737

Figure 3.